Ocean Sci. J. (2012) 47(4):497-508
http://dx.doi.org/10.1007/s12601-012-0045-z

Article

Available online at http://link.springer.com

SpringerLink

Ocean Science Journal

Paleomagnetic Records and Mineral-Magnetic Properties of Deep-Sea Sediments in the NW Pacific: Paleoenvironmental Implication

Cheong Kee Park[1]*, Wonnyon Kim[1], Youngtak Ko[1], Hyun-Bok Lee[1], Jai-Woon Moon[1], and Seong-Jae Doh[2]

[1]*Deep-sea and Seabed Resources Research Division, KIOST, Ansan 426-744, Korea*

[2]*Department of Earth and Environmental Sciences, College of Science, Korea University, Seoul 136-701, Korea*

Received 26 February 2012; Revised 20 August 2012; Accepted 14 October 2012

Abstract – The paleomagnetic records and mineral-magnetic properties of unconsolidated core sediment from the east Mariana Basin of the western Pacific have been analyzed to trace the time-dependent variations in sedimentary environments. Progressive alternating field demagnetization effectively extracts a stable remanent magnetization showing both normal and reverse polarities. Comparison of successive polarity changes, recorded in the sediment core, with reference magnetic polarity time-scale, reveals that the recovered sediment column was deposited since the late Pliocene. From the sediment age model, calculated sedimentation rate during the late Pliocene was 9.8 times higher than that during the Pleistocene. Considering the oceanic environments and geologic setting in the study area, the anomalous high sediment flux during the late Pliocene was probably caused by enhanced current flows, such as North Equatorial Current, associated with atmospheric circulation as well as by debris flows from adjacent sea mounts. In addition, the systematic variation of mineral-magnetic properties indicates periodical fluxes of coarse and magnetically stable particles, on the fine-grained dominant sedimentary environments. Such influxes, however, would not be related to syn-volcanic activities, because the summits of seamounts were totally blanketed by biogenic Pliocene–Pleistocene sediments. It is, hence, reasonable to interpret that paleomagnetic and mineral-magnetic data probably reflect drastic paleoenvironmental changes at the boundary between the Pliocene and Pleistocene, where strong current and atmospheric circulations decreased.

Key words – magnetostratigraphy, mineral-magnetic properties, paleoenvironment, Korea deep-sea research program

1. Introduction

In recent decades, the magnetic properties of deep-sea core sediments have provided essential paleoceanographic information and contributed to our understanding of global changes in the sedimentary environment. In particular, a combination of paleomagnetic and mineral-magnetic studies has identified temporal changes in the flux of eolian sediments and in the distribution of sediments in terms of bottom current intensities in the Pacific (Corliss and Hollister 1979; Ledbetter and Ellwood 1980; Doh 1989; Park et al. 2000; Sagnotti et al. 2001). For the deep-sea sediment cores, paleomagnetism and mineral-magnetism have also played vital roles in reconstructing the paleodepositional environments in terms of sedimentation ages and climate changes, based on the variations in paleomagnetic records and magnetic mineral properties, respectively (Crecelius et al. 1973; Chan et al. 1985; Joshima and Usui 1998; Oda et al. 2011).

Many studies have utilized the cores from the ODP (Ocean Drilling Project) and DSDP (Deep Sea Drilling Project) to reconstruct paleoceanographies, *inter alia* the evolution of seamounts, tectonic motions, and basin formation (e.g. Kamenetsky et al. 1997; Robertson 1998; Tandon et al. 1998; Mascle et al. 2001). In particular, data from Jurassic–Miocene rocks of the Northwest Pacific have provided important information on the evolution of seamounts, given the significant connections between sedimentary deposition and volcanic activity during those periods (Winterer and Metzler 1984; Lincoln et al. 1993).

Recently, the unconsolidated sediments of abyssal basins have attracted global interest as an important archive of biological, chemical, and physical records of fluctuations in productivity, the oceanic environment, and global climate (e.g. Martinet et al. 1997; Sabaa et al. 2004; Zhang et al. 2007; Li et al. 2011). In terms of mineral-magnetism,

*Corresponding author. E-mail: ckpark@kiost.ac

sediment cores are known to provide a stable record of ancient magnetic field variations (Freed and Healy 1974; Ledbetter and Ellwood 1980; Park et al. 2004) and abrupt climate changes, as deduced from changes in the properties of magnetic minerals (Worm and Weinreich 1988; Robinson et al. 2000; Sagnotti et al. 2001; Kissel et al. 2003; Dillon and Franke 2009).

The geological and hydrodynamic setting of the east Mariana Basin of the Northwest Pacific is marked by numerous Cretaceous volcanic seamounts (Menard 1984) and by the main passage of the North Equatorial Current (Lee et al. 2004). The current circulation is important in terms of sediment flux and climate change by heat-transport. In addition, the area is located in the northern boundary of the Western Pacific Warm Pool, which has the highest open-ocean water temperature (Yan et al. 1992). It has, therefore, experienced a series of biogenic and terrestrial material inputs, and has probably preserved an oscillation record in climate changes over millions of years. More importantly, sediments in the abyssal basin adjacent to the seamounts probably contain the periodic inputs of syn-volcanic debris from which the volcanic history of the seamounts can be postulated.

Magnetic techniques are useful to identify both the changes in sedimentary environments and paleoclimate by examining the sediment core (e.g. Thompson and Oldfield 1986; Maher et al. 2009). In addition, magnetic measurements can detect small changes in magnetic minerals (less than 1 μg/g) samples. Such high sensitivity enables magnetic measurements to discern and distinguish paleoclimate changes based on magnetic properties, including magnetic concentration, grain sizes, and mineralogy. In the present study, we obtained a sequential variation record of previous geomagnetic fields from sediment core collected in the abyssal basin, located between the seamounts of Ita Mai Tai and OSM 02, in the Northwest Pacific. Based on the down-core variations of mineral-magnetic properties, we try to clarify the factors controlling sedimentation, and their potential connection to climate change.

2. Sediment Core and Visual Description

The study area lies on the abyssal plain at an approximate depth of 6,000 m in the eastern part of the Mariana Basin, surrounded by the Marshall Islands to the east, the Mariana Islands to the west, and the Caroline Islands to the south (Fig. 1). The bathymetric map for the study area is based on a geophysical survey, using a multibeam echosounder (EM12), undertaken in 2000 on the R/V *Onnuri* during a scientific cruise to locate manganese crusts by the Korea Institute of Ocean Science and Technology (KIOST). A core sample was recovered from the abyssal basin between the Ita Mai Tai seamount (155.9°E, 12.9°N) and the OSM 02 seamount (157.6°E, 13.9°N) (Fig. 1). These seamounts exhibit subconical-shaped guyots, typical of seamounts in the western Pacific (Watkins et al. 1995; Mel'nikov et al. 2010). The recovered core, 3.6 m long, was split in two longitudinally. The half sediment archive was used to provide a visual core description of the vertical sedimentary profile in terms of bioturbation, sediment color and grain-size amongst other things and then kept for further measurements.

The vertical section from the sediment archive is illustrated and described in Fig. 2. The sediments display an alternating assortment of brown-series colors. Based on the Munsell Soil Color Chart (1975), the colors are designated as dark brown (10YR3/3), brown (10YR4/3), dark yellowish brown (10YR3/4–6), and yellowish brown (2.5YR5/4).

The upper part of the section (0–30 cm) consists of homogeneous dark-brown mud with several mottled patches. The intervals at 30–40, 172–177, and 210–217 cm consist of intensively mottled and bioturbated sediment. Lenticular lamination is highly developed in the lower section at intervals of 227–265.5 and 300–348 cm, indicating strong bottom-current activity (Viana et al. 1998; Park et al. 2000; Wynn and Stow 2002). On the other hand, the upper and middle parts of the section above ~227 cm were probably deposited in a relatively gentle and steady sedimentary environment.

3. Magnetic Methods

For magnetic measurements, a total of 157 samples were excavated from the core at a regular space (~2.3 cm) using plastic non-magnetic cubes (2 × 2 × 2 cm). After weighing, all samples were subjected to various magnetic experiments and measurements including: low-field magnetic susceptibility (χ_{LF}), alternative field (AF) demagnetization, anhysteretic remanent magnetization (ARM), and stepwise acquisition of isothermal remanent magnetization (IRM).

χ_{LF} was measured with a Bartington Instruments MS1B magnetic susceptibility meter at a frequency of 0.47 kHz. After measurements of natural remanent magnetization (NRM), several pilot samples were selected based on lithological

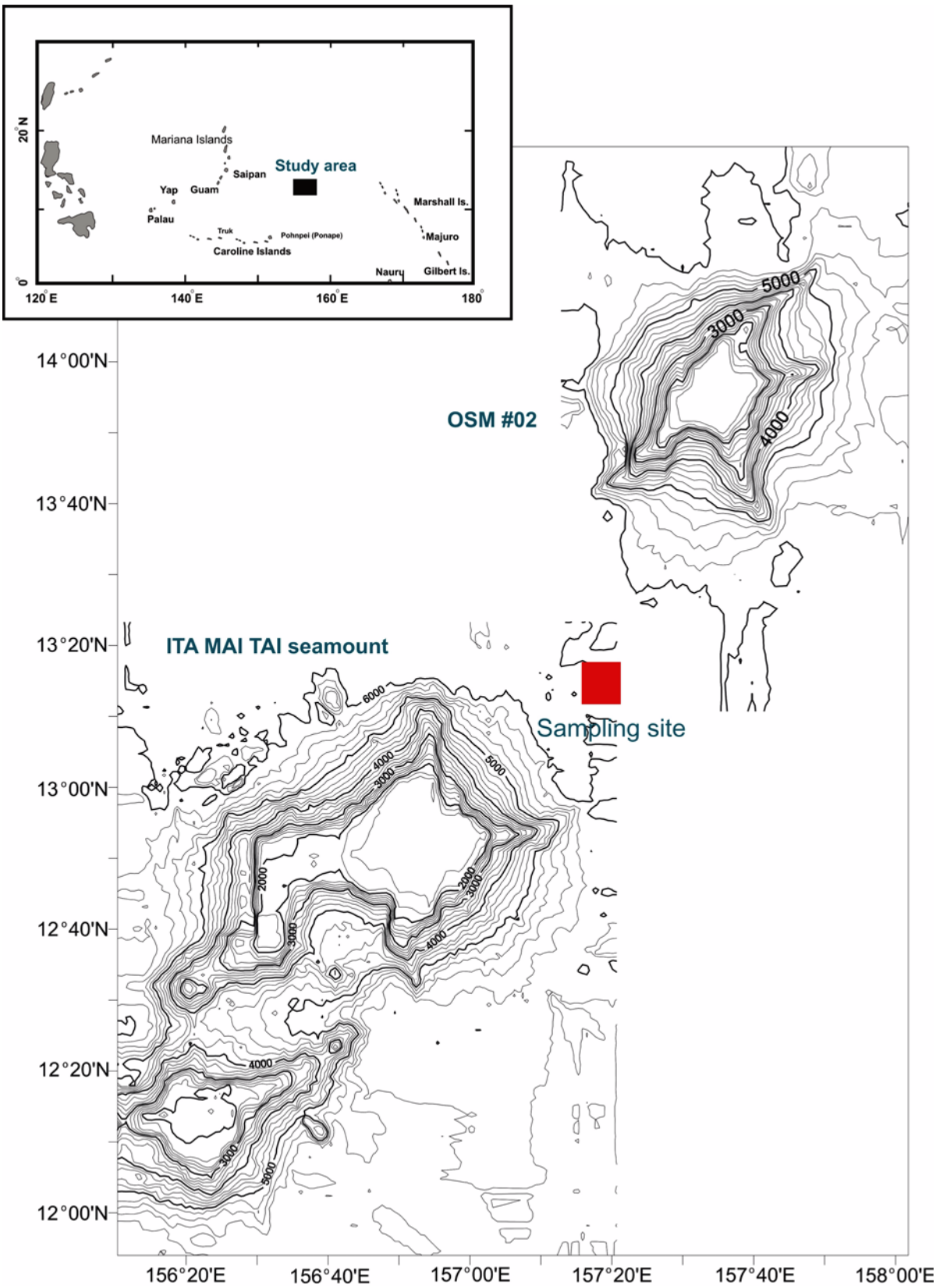

Fig. 1. Topographic map of the study area. The sampling site is located between the seamounts of Ita Mai Tai and OSM 02 with water depths ~6,000 m. The bathymetry was obtained from the multibeam echosounder (EM12) survey performed in 2000 by KORDI

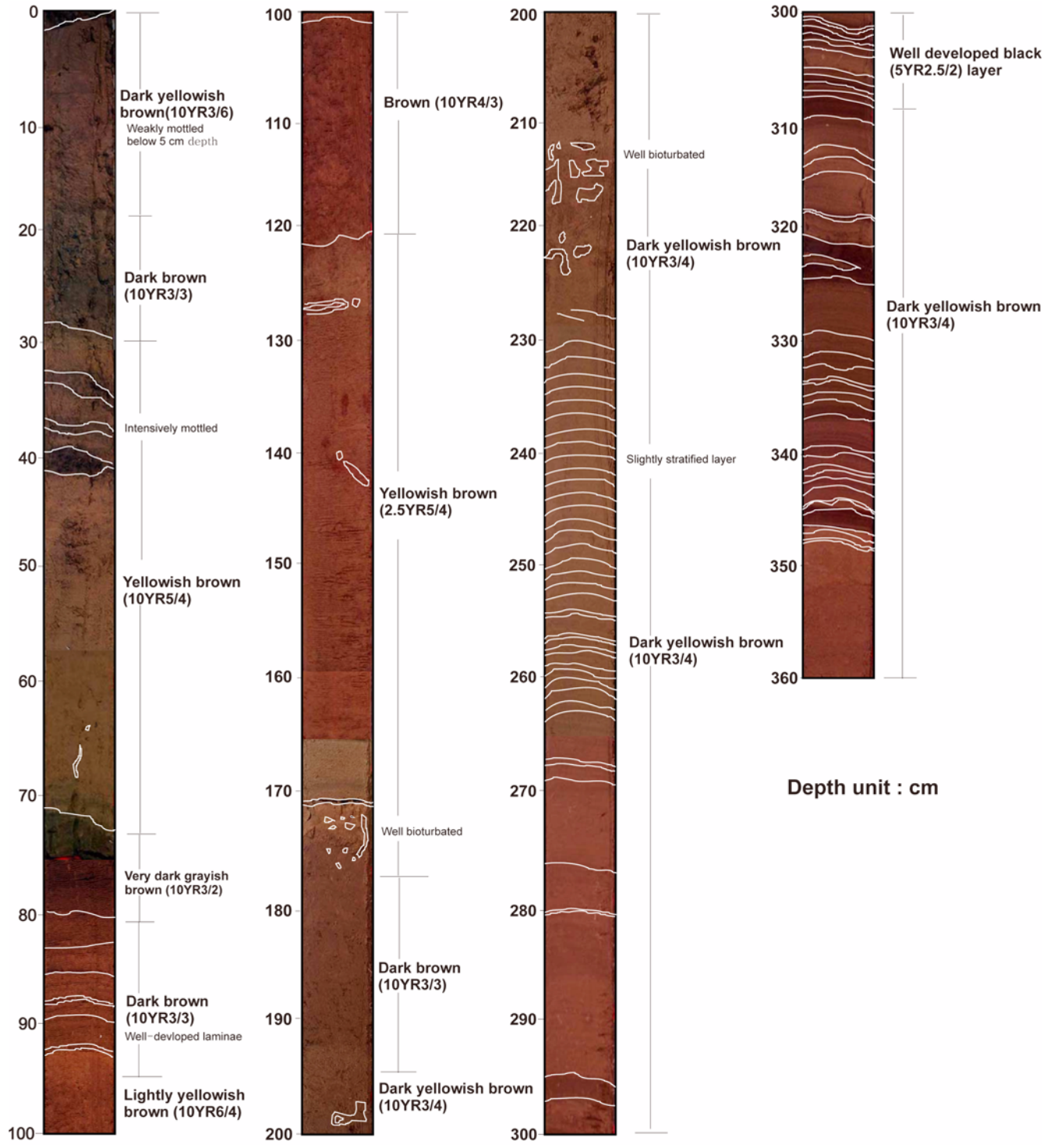

Fig. 2. Visual descriptions of archived sediments including distinctive sedimentary layers, bioturbation, and color. Color was determined from the Munsell Soil Color Chart (1975)

characteristics, such as variations in sediment color and facies. For the pilot samples, stepwise AF demagnetization experiments were performed on a Molspin AF demagnetizer with increasing AF levels (5, 7.5, 10, 15, 17.5, 20, 25, 30, 40, 50, 60, 70, 80, and 90 mT). According to the results of the pilot experiments, the remaining samples were demagnetized

through four or five successive AF steps (17.5, 20, 25, and 30 mT). The ARM was induced using a Molspin AF demagnetizer with ARM attachment at a peak AF of 90 mT, with a steady 0.05 mT direct current (DC) field superimposed. IRM acquisition experiments were performed in a stepwise manner increasing DC fields up to 2.5 T, using an ASC Scientific IM-10-30 impulse magnetizer. For convenience, an IRM of 2.5 T imparted on a sample is regarded here as saturation IRM (SIRM). At saturation, a DC field of 0.3 T was then applied in the opposite direction ($IRM_{-0.3T}$).

All the remanence measurements were made on a Molspin spinner magnetometer. Throughout the measurements, all the samples were stored in a magnetic-field free space to prevent subsequent acquisition of viscous magnetization. The measurements were used to obtain various magnetic parameters and interparametric ratios in connection with magnetic concentration (χ_{LF}, ARM, and SIRM), grain-size (ARM/χ_{LF}), and for the relative ease of swapping the coercivity polarities ($HIRM\% = 50(SIRM + IRM_{-0.3T})/SIRM$; S ratio = $-IRM_{-0.3}/SIRM$).

Mineral-magnetic parameters are commonly applied as indices to trace the changes in depositional environment and paleoclimate in terms of the concentration, grain-size, and mineralogy of the magnetic minerals in sediment cores (e.g. Verosub and Roberts 1995; Sagnotti et al. 2001; Deng et al. 2006). Of the various magnetic parameters, the values of χ_{LF}, ARM, and SIRM show an approximately linear dependence on the concentration of magnetic minerals in a sample (e.g. Thompson and Oldfield 1986; Robinson 1990; Bloemendal et al. 1993; Evans and Heller 2003). In particular, ARM is sensitive to fine grains (<1 μm), while χ_{LF} and SIRM respond to various sizes of magnetic minerals (e.g., Maher, 1988; Evans and Heller, 2003). Hence, ARM/χ_{LF} is widely used as a grain-size proxy, so that higher values of ARM/χ_{LF} indicate a finer average grain-size in the sample. For the magnetic mineralogy deduced from coercivities, HIRM and S ratios are effective in determining the relative abundance of high-coercivity magnetic minerals (hematite and/or goethite) and low-coercivity magnetic minerals (magnetite), respectively. For instance, magnetite-dominant samples have low HIRM and high S ratios.

4. Results

AF demagnetization experiments

All the prepared samples show stable characteristic remanent magnetizations (ChRMs) in the progressive AF demagnetization experiments. Typical AF demagnetizations are displayed in vector projections (Fig. 3). In this diagram, the base of the NRM vector is placed at the origin of a Cartesian coordinate system, and the tip of the vector is projected onto two orthogonal planes. The distance of each data point from the origin is a measure of the total intensity of magnetization (Zijderveld 1967).

Most samples show two distinct and separable magnetization components. In general, soft viscous or unstable components are characterized by rapid changes in direction and removed at the AF of about 5–10 mT (Fig. 3). After removal, a well-defined ChRM, converging towards the origin, is revealed at more than five AF steps between 15–90 mT with the maximum angular deviation being <10° (Fig. 3). The ChRMs show almost opposing directions, as seen by the flip-flop of declinations in the vector diagrams indicating alternative downcore variation of magnetic polarity.

The unconsolidated sediment samples probably acquired detrital remanent magnetization, but the observed ChRM directions would not be distorted by inclination error (i.e., inclination shallowing) because deep-sea or slowly deposited lake sediments are free from inclination error (Tauxe et al., 2006). In particular, inclination error is negligible at low-latitudes, as the result of a laboratory re-deposition experiment (Tauxe and Kent, 1984). Hence, we considered the obtained ChRMs reflected well the previous geomagnetic directions.

Paleomagnetic age dating

The detection of changes in magnetic polarity in the present samples relied on variations in magnetic declination, because of less distinctive inclinational changes at a low latitude (13.15°N). In practice, a change in polarity in the down-core sediments was determined by an almost 180° flip in declination. Technically, the sediment core could not be oriented with respect to the azimuth due to the extreme depth of the sea-bottom (~6,000 m). Hence, the declinations of the uppermost samples are corrected to be in line with the expected declination of the current geomagnetic field (4.44°) at the sampling site (http://wdc.kugi.kyoto-u.ac.jp/igrf/index.html). The observed successive declinations are then presented as relative values (Fig. 4). It is notable that the inclinations in the surface sediment layer are similar to the inclination of the current geomagnetic field (13.12°), indicating that the retrieved samples are well preserved magnetic signals. Down-core variation of inclinations also

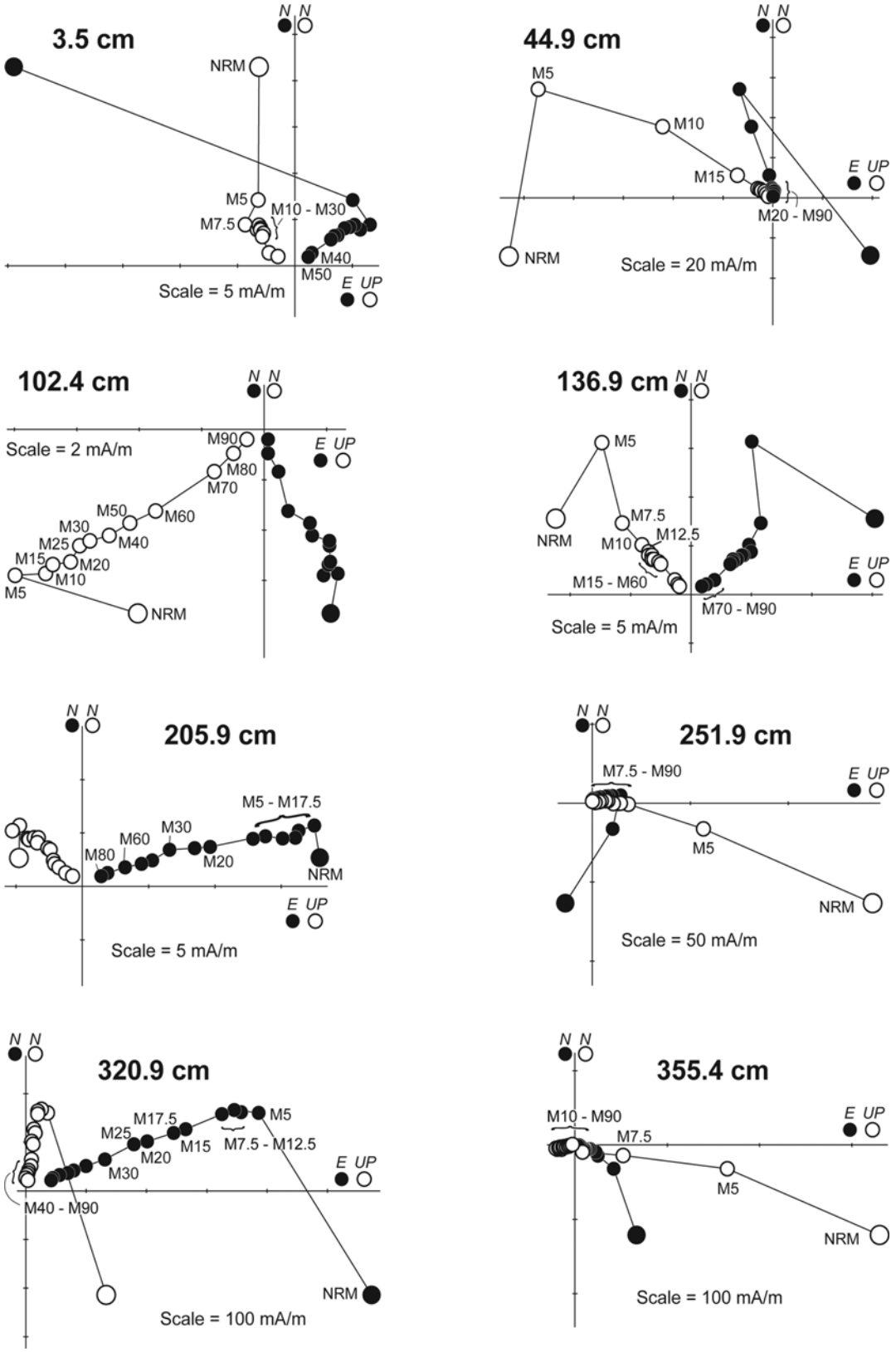

Fig. 3. Progressive alternating field (AF) demagnetization behavior in vector projections (Zijderveld, 1967) of representative samples. The diagram shows the declinational variations (solid symbols) on the horizontal plane and the inclinational variations (open symbols) on the vertical plane. The axes are the magnetization and the scale is shown below the horizontal axis

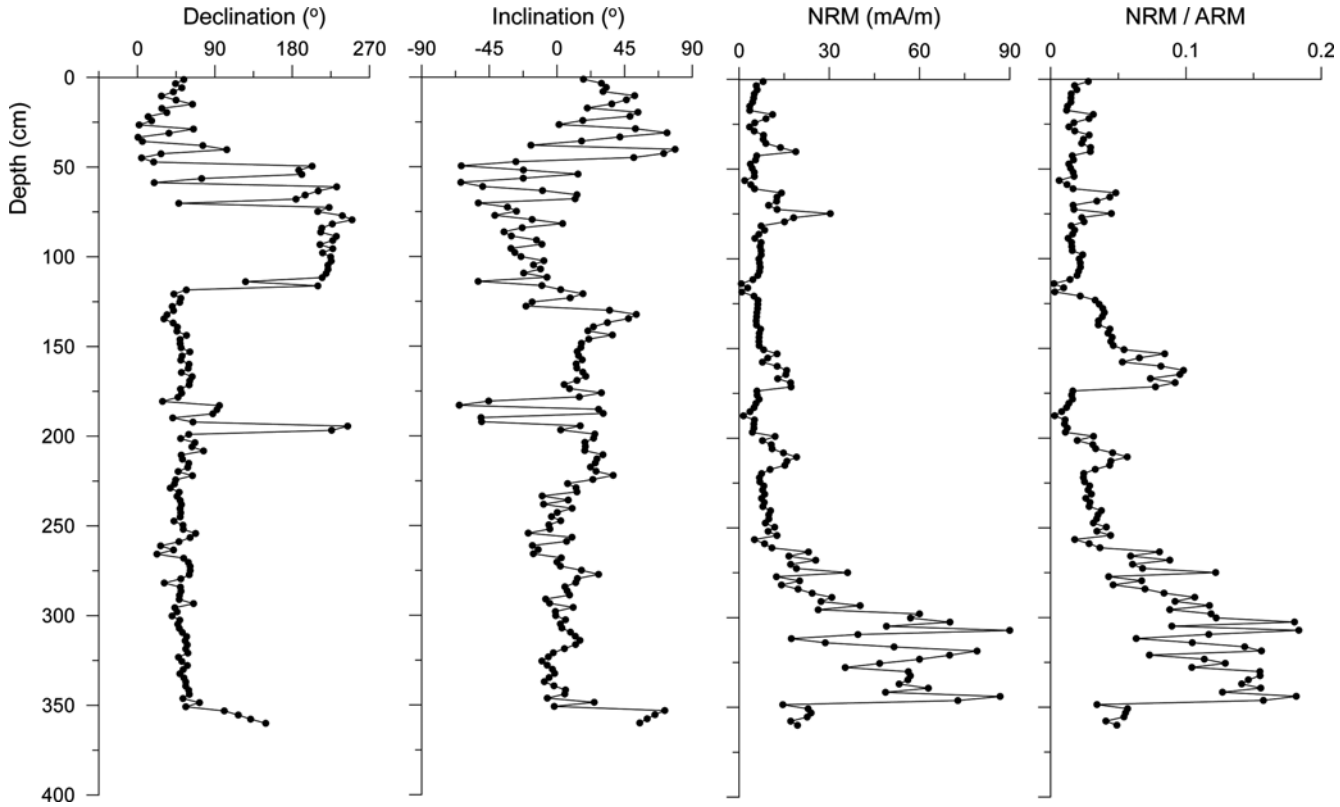

Fig. 4. Vertical profiles of paleomagnetic directions (declination and inclination), intensities of natural remanent magnetization (NRM), and relative geomagnetic field intensity (NRM/anhysteretic remanent magnetization (ARM)). Because the sampling site is located at the low latitude, the directional changes are more distinctive in declination

shows distinctive polarity changes, similar to the declinations (Fig. 4). In the present study, four distinctive polarity changes are detected above the 200 cm horizon, where the sedimentary depositional environment was characteristically gentle and steady (see Section 2). On the other hand, only one change of polarity occurs in the lower part of the sediment core.

The magnetic polarity sequences (Fig. 5) were determined by matching the patterns to those of the geomagnetic polarity timescale of Gradstein et al. (2004). The boundary between Brunhes Normal and Matuyama Reverse Chron (0.78 Ma) is found at ~48.3 cm. The Jaramillo Normal Subchron (0.99–1.07 Ma) occurs between the core depths of 55.2 and 59.8 cm, and is depicted as C1r.1n (Fig. 5). Although the reference geomagnetic polarity timescale excludes the Cobb Normal cryptochron (1.17–1.19 Ma), because it is regarded as a local non-dipolar geomagnetic field variation (Gradstein et al., 2004), our magnetic data detected this as a very short normal chron (C1r.2n) at a depth of 69.0–71.3 cm. The preservation of such a short-term geomagnetic variation event in the core sediments is supporting evidence for the gentle and steady depositional environment that we suggested for the upper part of the core (in Section 2). At depths of 117.3–193.3 cm, the sediment samples exhibit a normal polarity that can be correlated with the Olduvai Normal subchron (1.78–1.95 Ma). Finally, a normal polarity is maintained throughout the relatively long section of core from depths of 197.9 to 356.6 cm, and this can be assigned to the Reunion normal event (2.13–2.15 Ma), which is the first normal event within the Matuyama Reverse Chron (Gradstein et al. 2004).

Mineral-magnetic properties

Fig. 6 shows vertical profiles of concentration-dependent magnetic parameters (χ_{LF}, ARM, and SIRM) and a grain-size proxy (ARM/χ_{LF}). All the concentration-related magnetic parameters show similar down-core variations with the apices of χ_{LF} (101.0–297.2 × 10^{-8} m^3/kg), ARM (365.9–958.6 × 10^{-8} Am^2/kg) and SIRM (346.4–1460.5 × 10^{-5} Am^2/kg) in the upper and lower parts of the section, indicating a

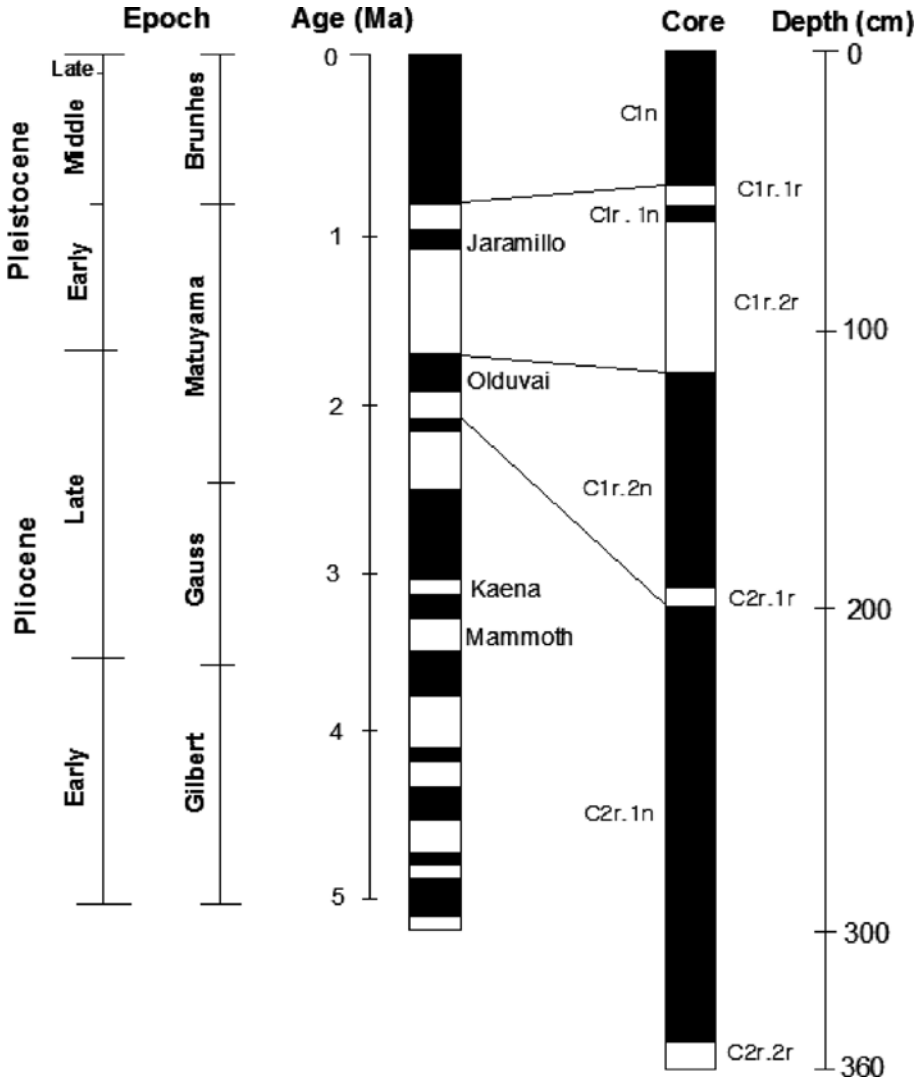

Fig. 5. Magnetostratigraphic correlation for the core sample. The black and white intervals indicate normal and reverse polarities, respectively. The central column is the reference geomagnetic time scale (Gradstein et al. 2004)

significant influx of magnetic minerals. On the other hand, comparatively low values, except a small peak at the depths of 180–195 cm, are maintained in the middle part of the section (100–290 cm). For instance, χ_{LF} fluctuates subsequently until the depth of 95 cm showing the values of 26.93–297.24 × 10^{-8} m^3/kg. Below the 95cm horizon, moderate χ_{LF} values ranging from 40 to 100 × 10^{-8} m^3/kg are maintained and then followed by an abrupt increase to 292.23 × 10^{-8} m^3/kg at the depth of ~300 cm. Throughout the core, notable peaks of magnetic concentrations (higher values of χ_{LF}, ARM, and SIRM) are observed at the depths of 20–42, 70–95, 180–195, and 295–360 cm in which dark-brown colored sediments are dominant (see Fig. 2).

The down-core variation in ARM/χ_{LF} presents almost a mirror image to those of χ_{LF}, ARM, and SIRM especially in the upper and lower parts of the section (Fig. 6). The values of ARM/χ_{LF} are also highly responsive to changes in the color of the sediment; comparatively low, a dominance of coarse-grained magnetic minerals, in dark-brown colored layers. In detail, ARM/χ_{LF} values of dark-brown sediments are in the range 2.6–4.9 × 10^{-6} A/m, while those of brown sediments are relatively high, varying from 4.7 to 7.6 × 10^{-6} A/m. In relation to the content of magnetic minerals, these results imply that the coarser magnetic grains are highly concentrated in the darker-colored sedimentary layers (i.e., corresponding to the apices of χ_{LF}, ARM, and SIRM, and the lower values of ARM/χ_{LF}).

The maximum coercivity for magnetite is 0.3 T, whereas

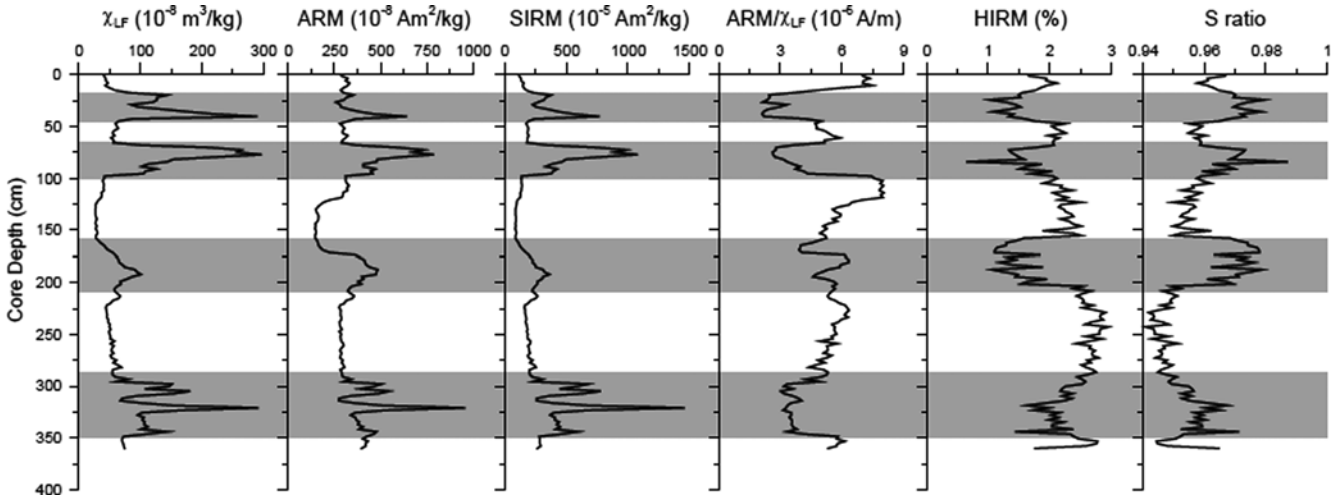

Fig. 6. Vertical profiles of mineral-magnetic parameters, including magnetic concentration (χ_{LF}, ARM, and SIRM), grain-size (ARM/χ_{LF}), and relative abundance of high- and low-coercivity minerals (HIRM and S ratio, respectively). High values of ARM/χ_{LF} indicate finer mean magnetic grain-size

for hematite and goethite it is much higher than 0.3 T. The value of the S ratio for magnetite is therefore close to 1.0. Throughout the sediment core, the values of S ratios are higher than 0.94, indicating the dominance of low-coercivity magnetite-like minerals. In addition, comparatively higher values occur in the same parts of the section as the apices of χ_{LF}, ARM, and SIRM, and the lower values of ARM/χ_{LF} (Fig. 6). Overall, the mineral-magnetic properties of the sediment core indicate that the depositional environment in the study area was marked by occasional notable fluxes of coarse-grained magnetite-like minerals into the prevailing fine-grained sedimentary setting. The coarse-grain fluxes were more distinctive in the upper and lower parts of the sediment core.

5. Discussion

In this study, we have described the vertical variations of paleomagnetic records and mineral-magnetic properties preserved in a sediment archive of the northwestern Pacific abyssal plain. The variations indicate temporal changes in the depositional environment, including changes in the regional sedimentary input and climate change. Given the complexity of seamount evolution in the vicinity of the study area (Wedgeworth and Kellogg 1987; Lee et al. 2003), it is very important to investigate the sources of the input sediments.

In general, non-fossiliferous pelagic clays in the northern Pacific region are known to be magnetically unstable (Yamazaki and Katsura 1990). In particular, the presence of less-stable magnetic minerals in dark brown sediments can be caused by the selective dissolution of magnetic minerals (Park et al. 2000). On the other hand, the results of our paleomagnetic investigations show that the core sediments have a stable remanent magnetization (Fig. 4). The directional changes, deduced both from declination and inclination, also reflect the changes in the polarity of the Earth's magnetic field. Compared to the reference geomagnetic polarity timescale, the ages of the recovered sediment core range from the late Pliocene through the Pleistocene (Fig. 7). The average sedimentation rate for the Pleistocene (from the Brunhes Normal Chron to the topmost Olduvai Normal Subchron) is calculated to be 0.66 mm/10^3 year. In contrast, for the late Pliocene, the average sedimentation rate is estimated to be 6.47 mm/10^3 year, 9.8 times higher than that in the Pleistocene (Fig. 7), indicating notable sediment flux during the late Pliocene. The depositional environments of the Pacific region, during the late Pliocene and Pleistocene, can be summarized in terms of global climatic oscillations involving polar cooling, variation of ocean-circulation intensity, and Pleistocene glaciations (Corliss and Hollister 1979; Prince et al. 1980; Rea and Janecek 1982). Considering these paleoenvironmental factors, large amounts of sediments could be transported to the deep ocean floor by strong winds and/or active bottom currents (e.g., Corliss and Hollister 1979). Because the study area

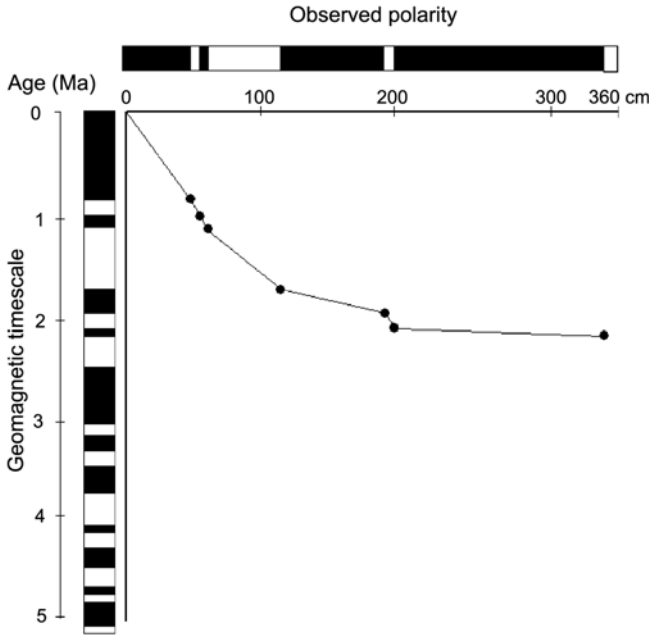

Fig. 7. Plot of the magnetic polarity change obtained in the sediment core versus the reference geomagnetic time scale. Sedimentation rates are calculated by the ratio of sediment thickness to the corresponding geological time. The average sedimentation rate for the late Pliocene was ~10 times higher than that for Pleistocene. See the enormous volume of sediment flux at ~2 Ma

was exerted as the main passage of the North Equatorial Current (Lee et al. 2004), the strong current flows probably carried enormous sediments to the study area especially before the Pleistocene glaciation.

As the other sediment source, debris flows from the adjacent seamounts can be important. In general, the values of χ_{LF}, ARM, and SIRM are proportional to the concentration of magnetic particles in sediments, and furthermore, their fluctuations reflect well the change in sediment flux intensity and/or sediment source (Hartstra 1982; Oldfield and Yu 1994; Walden et al. 1997; Hounslow and Morton 2004; Maher et al. 2009). As shown in Figs. 2 and 6, the drastically fluctuating trends of χ_{LF}, ARM, and SIRM have the main apices observed in the darker colored upper parts of the core section and in the highly laminated lower part of the section. Compared to the variation of a magnetic grain-size parameter (ARM/χ_{LF}), the horizons showing higher values of concentration-related magnetic parameters (χ_{LF}, ARM, and SIRM) are correlated well with those of lower ARM/χ_{LF} values (see Fig. 6). Such correlation indicates the occasional fluxes of coarse-grained sediments containing relatively large amount of magnetic minerals. In addition, the coarse grain-size (i.e. low ARM/χ_{LF} value) implies short-range transport rather than long-range transport by bottom currents. As shown in Fig. 1, the study area is located between the Ita Mai Tai and OSM 02 seamounts. From these seamounts, periodic debris flows probably left their magnetic mark in the study area. However, debris flows were not of syn-volcanic origin, because volcanic activity has ceased completely since the Eocene (Jackson and Schlanger 1976; Wedgeworth and Kellogg 1987) and the summits of the seamounts were completely blanketed by biogenic sediments since the Pliocene (Mel'nikov et al. 2010).

Overall, sedimentation history in the study area can be successfully uncovered, based on the paleomagnetic and mineral-magnetic data. During the late Pliocene, a large volume of fine-grained sediments, indicating long-range transport, was carried by the strong bottom current flows. In such a sedimentary environment, occasional debris flows supplied coarse-grained sediments from the adjacent seamounts. At the beginning of the Pleistocene glaciation, supplement of fine-grained sediments decreased dramatically, implying a weakening of the current flows, such as the North Equatorial Current. In relays, the range of the Western Pacific Warm Pool was also reduced to near the equator (Yan et al. 1992). As a result, small amounts of sediments were supplied only from the adjacent seamounts in forms of debris flows during the Pleistocene.

6. Conclusion

Within the framework of paleoceanography, the late Pliocene and Pleistocene are characterized by the onset of northern glaciations and consequential climatic deterioration. Around the boundary of the late Pliocene/Pleistocene, the large differences in global temperature resulted in intensified atmospheric and oceanic circulations, accelerating the sediment supplements to the deep ocean floor. Such global climate change also influenced the sedimentary environments in the study area. Paleomagnetic data suggest that the ages of the recovered sediment core range from the late Pliocene through the Pleistocene. The average sedimentation rate for the late Pliocene was ~10 times higher than that for Pleistocene, probably due to enhanced circulation of bottom currents, such as the North Equatorial Current. The long-range sediment transport produced a fine-grained sedimentary setting. On the other hand, mineral-magnetic data showed occasional fluxes of coarse-grained sediments from the

adjacent seamounts, the Ita Mai Tai and OSM 02 seamounts. The sediments, however, were not related to volcanic activity, because the summits of seamounts were totally blanketed by biogenic Pliocene–Quaternary sediments (Mel'nikov et al. 2010).

Acknowledgments

This research was supported by the Ministry of Land, Transport, and Maritime Affairs of Korea (PM56281) and KORDI (PE98662). This manuscript was greatly improved by the constructive comments and suggestions made by two anonymous reviewers, as well as by the journal editor, Dr. W.J. Shim.

References

Bloemendal J, King JW, Hunt A, deMenocal PB, Hayashida A (1993) Origin of the sedimentary magnetic record at Ocean Drilling Program sites on the Owen ridge, western Arabian sea. J Geophys Res **98**:4199-4219

Chan LS, Chu CL, Ku TL (1985) Magnetic stratigraphy observed in ferromanganese crust. Geophys J Roy Astronomic Soc **80**:715-723

Corliss BH, Hollister CD (1979) Cenozoic sedimentation in the central north Pacific. Nature **282**:707-709

Crecelius EA, Carpenta R, Merrill RT (1973) Magnetism and magnetic reversals in ferromanganese nodules. Earth Planet Sci Lett **17**:391-396

Deng C, Shaw J, Liu Q, Pan Y, Zhu R (2006) Mineral magnetic variation of the Jingbian loess/paleosol sequence in the northern Loess Plateau of China: Implication for Quaternary development of Asian aridification and cooling. Earth Planet Sci Lett **271**:248-259

Dillon M, Franke C (2009) Diagenetic alteration of natural Fe–Ti oxides identified by energy dispersive spectroscopy and low-temperature magnetic remanence and hysteresis measurements. Phys Earth Planet Inter **172**:141-156

Doh SJ (1989) Stratigraphic and sedimentological implications of rock-magnetic properties of marine sediments from the northwest Pacific. J Geol Soc Korea **25**:137-151

Evans ME, Heller F (2003) Environmental magnetism: Principles and applications of enviromagnetics. Academic Press, Oxford

Gradstein F, Ogg J, Smith A (2004) A geologic time scale. Cambridge University Press, Cambridge

Hartstra RL (1982) Grain-size dependence of initial susceptibility and saturation magnetization-related parameters of four natural magnetitites in the pseudo-single domain–multidomain range. Geophys J Roy Astronomic Soc **71**:477-495

Hounslow MW, Morton AC (2004) Evaluation of sediment provenance using magnetic mineral inclusions in clastic silicates: Comparison with heavy mineral analysis. Sediment Geol **171**:13-36

Jackson ED, Schlanger SO (1976) Regional syntheses, Line Islands Chain, Tuomato Island Chain, and Manihiki Plateau, Central Pacific Ocean. Initial Reports DSDP **33**:915-927

Joshima M, Usui A (1998) Magnetostratigraphy of hydrogenetic manganese crusts from northwestern Pacific seamounts. Mar Geol **146**:53-62

Kamenetsky VS, Crawford AJ, Eggins S, Muhe R (1997) Phenocryst and melt inclusion chemistry of near-axis seamounts, Valu Fa Ridge, Lau Basin: Insight into mantle wedge melting and the addition of subduction components. Earth Planet Sci Lett **151**:205-223

Kissel C, Laj C, Clemens C, Solheid P (2003) Magnetic signature of environmental changes in the last 1.2 Myr at ODP Site 1146, South China Sea. Mar Geol **201**:119-132

Ledbetter MT, Ellwood BB (1980) Spatial and temporal changes in bottom-water velocity and direction from analysis of particle size and alignment in deep-sea sediment. Mar Geol **38**:245-261

Lee SY, Huh CA, Su CC, You CF (2004) Sedimentation in the southern Okinawa trough: Enhanced particle scavenging and teleconnection between the equatorial Pacific and western Pacific margins. Deep-Sea Res I **51**:1769-1780

Lee TG, Lee SM, Moon JW, Lee KH (2003) Paleomagnetic investigation of seamounts in the vicinity of Ogasawara Fracture Zone northwest of the Marshall Islands, western Pacific. Earth Planet Space **55**:355-360

Li L, Li Q, Tian J, Wang P, Wang H, Liu Z (2011) A 4-Ma record of thermal evolution in the tropical western Pacific and its implications on climate change. Earth Planet Sci Lett **309**:10-20

Lincoln JM, Pringle MS, Silva P (1993) Early and Late Cretaceous volcanism and reef-building in the Marshall Islands. In: Pringle MS, Sager WW, Silter WV, Stein S (eds) The Mesozoic Pacific. American Geophysical Union, Geophysical Monograph Series **77**:1-435

Maher BA (1988) Magnetic properties of some synthetic submicron magnetite. Geophys J Int **94**:83-96

Maher BA, Watkins SJ, Brunskill G, Alexander J, Fielding CR (2009) Sediment provenance in a tropical fluvial and marine context by magnetic 'fingerprinting' of transportable sand fractions. Sedimentology **56**:841-861

Mascle GH, Tricart P, Torelli L, Bouillin JP, Rolfo F, Lapierre H, Monié P, Depardon S, Mascle J, Peis D (2001) Evolution of the Sardinia Channel (Western Mediterranean): New constraints from a diving survey on Cornacya seamount off SE Sardinia. Mar Geol **179**:179-201

Mel'nikov ME, Tugolesov DD, Pletnev SP (2010) The structure of the incoherent sediments in the Ita Mai Tai guyot (Pacific

Ocean) based on geoacoustic profiling data. Oceanology **50**: 582-590

Menard HW (1984) Darwin reprise. J Geophys Res **89**:9960-9968

Munsell Soil Color Charts (1975) Munsell Soil Color Charts. Kollmorgen, Baltimore

Oda H, Usui A, Miyagi I, Joshima M, Weiss BP, Shantz C, Fong LE, McBride KK, Harder R, Baudenbacher FJ (2011) Ultrafine-scale magnetostratigraphy of marine ferromanganese crust. Geology **39**:227-230

Oldfield F, Yu L (1994) The influence of particle size variations on the magnetic properties of sediments from the north-eastern Irish Sea. Sedimentology **41**:1093-1108

Park CK, Doh SJ, Suk DW (2000) Sedimentary fabric on deep-sea sediments from KODOS area in the eastern Pacific. Mar Geol **171**:115-126

Park CK, Son SK, Kim KH, Chi SB, Doh SJ (2004) Paleomagnetic results from deep-sea sediment of the Korea Deep Ocean Study (KODOS) area (northern equatorial Pacific) and their paleodepositional implications. Geo-Mar Lett **24**:112-124

Prince RA, Heath GR, Kominz M (1980) Paleomagnetic studies of central north Pacific sediments cores: Stratigraphy, sedimentation rates, and the origin magnetic instability: Summary. Geol Soc Am Bull **91(II)**:1789-1835

Rea DK, Janecek TR (1982) Late Cenozoic changes in atmospheric circulation deduced from north Pacific eolian sediments. Mar Geol **49**:185-206

Robertson AHF (1998) Tectonic significance of the Eratosthenes Seamount: A continental fragment in the process of collision with a subduction zone in the eastern Mediterranean (Ocean Drilling Program Leg 160). Tectonophysics **298**:63-82

Robinson SG (1990) Applications for whole-core magnetic susceptibility measurements of deep-sea sediments: Leg 115 results. Proc ODP **115**:737-771

Robinson SG, Sahota JTS, Oldfield F (2000) Early diagenesis in North Atlantic abyssal plain sediments characterized by rock-magnetic and geochemical indices. Mar Geol **163**:77-107

Sabaa AT, Sikes EL, Hayward BW, Howard WR (2004) Pliocene sea surface temperature changes in ODP Site 1125, Chatham Rise, east of New Zealand. Mar Geol **205**:113-125

Sagnotti L, Macri P, Camerlenghi A, Rebesco M (2001) Environmental magnetism of Antarctic Late Pleistocene sediments and interhemispheric correlation of climatic events. Earth Planet Sci Lett **192**:65-80

Tandon K, Lorenzo JM, de La Linde Rubio J (1998) Timing of rifting in the Alboran Sea basin - correlation of borehole (ODP Leg 161 and Andalucia A-1) to seismic reflection data: Implications for basin formation. Mar Geol **144**:275-294

Tauxe L, Kent DV (1984) Properties of a detrital remanence carried by hematite from study of modern river deposits and laboratory redeposition experiments. Geophys J Roy Astronomic Soc **76**:543-561

Tauxe L, Steindorf JL, Harris A (2006) Depositional remanent magnetization: Toward an improved theoretical and experimental foundation. Earth Planet Sci Lett **244**:515-529

Thompson, R, Oldfield F (1986) Environmental Magnetism. Allen and Unwin, London

Verosub KL, Roberts AP (1995) Environmental magnetism: Past, present, and future. J Geophys Res **100(B2)**:2175-2192

Viana AR, Faugeres JC, Stow DAV (1998) Bottom-current-controlled sand deposits: A review of modern shallow- to deep-water environments. Sediment Geol **115**:53-80

Walden J, Slattery MC, Burt TP (1997) Use of mineral magnetic measurements to fingerprint suspended sediment sources: Approaches and techniques for data analysis. J Hydrol **202**: 353-372

Watkins DK, Pearson PN, Erba E, Rack FR, Silva IP, Bohrmann HW, Fenner J, Hobbs PRN (1995) Stratigraphy and sediment accumulation patterns of the upper Cenozoic pelagic carbonate caps of guyots in the northwestern Pacific Ocean. Proc ODP Sci Result **144**:675-689

Wedgeworth B, Kellogg J (1987) A 3-D gravity-tectonic study of Ita mai tai guyot: An uncompensated seamount in the east Mariana Basin. In: Keating BH, Fryer P, Batiza R, Boehlert GW (eds) Seamounts, Islands, and Atolls. American Geophysical Union, Geophysical Monograph Series **43**:73-95

Winterer EL, Metzler CV (1984) Origin and subsidence of Guyots in mid-Pacific Mountains. J Geophys Res **89**:9969-9979

Worm HU, Weinreich N (1988) Rock magnetism of pelagic sediments from the Equatorial Pacific. Earth Planet Sci Lett **89**:184-192

Wynn RB, Stow DAV (2002) Classification and characterisation of deep-water sediment waves. Mar Geol **192**:7-22

Yamazaki T, Katsura T (1990) Magnetic grain size and viscous remanent magnetization of pelagic clay. J Geophys Res **95**: 4373-4382

Yan X-H, Ho CR, Zheng Q, Klemas V (1992) Temperature and size variabilities of the western Pacific warm pool. Science **258**:1643-1645

Zhang J, Wang P, Li Q, Cheng X, Jin H, Zhang S (2007) Western equatorial Pacific productivity and carbonate dissolution over the last 550 kyr: Foraminiferal and nannofossil evidence from ODP Hole 807 A. Marine Micropaleontol **64**:121-140

Zijderveld JDA (1967) A.C. demagnetization of rocks: Analysis of results, In: Collinson DW, Creer KM, Runcorn SK (eds) Methods in Palaeomagnetism. Elsevier, Amsterdam